THE JOURNAL OF BIOLOGICAL CHEMISTRY VOL. 287, NO. 19, pp. 15557–15569, May 4, 2012

Possible Role of Efnb1 Protein, a Ligand of Eph Receptor Tyrosine Kinases, in Modulating Blood Pressure*

Received for publication, February 6, 2012, and in revised form, March 1, 2012 Published, JBC Papers in Press, March 5, 2012, DOI 10.1074/jbc.M112.340869

Zenghui Wu[‡1], Hongyu Luo[‡1], Eric Thorin[§], Johanne Tremblay[‡], Junzheng Peng[‡], Julie L. Lavoie[‡], Yujia Wang[‡], Shijie Qi[‡], Tao Wu[‡¶2], and Jiangping Wu[‡‖3]

From the [‖]Nephrology Department and [‡]Centre de Recherche, Centre Hospitalier de l'Université de Montréal (CRCHUM), Montreal, Quebec H2L 4M1, Canada, [§]Montreal Heart Institute, Montreal, Quebec H1T 1C8, Canada, and [¶]Institute of Cardiology, the First Affiliated Hospital, Medical College, Zhejiang University, 310003 Hangzhou, China

Background: Currently, there is no knowledge about the function of ephrins in vascular smooth muscle contraction and blood pressure regulation.
Results: Stimulating Efnb1 reduces vascular smooth muscle cell contraction. Efnb1 null mutation increases RhoA activation and heightens blood pressure in mice.
Conclusion: Efnb1 can regulate vessel tone and blood pressure.
Significance: We identified a new group of molecules capable of regulating blood pressure.

Eph kinases constitute the largest receptor tyrosine kinase family, and their ligands, ephrins (Efns), are also cell surface molecules. Although they are ligands, Efns can transduce signals reversely into cells. We have no prior knowledge of the role played by any members of this family of kinases or their ligands in blood pressure (BP) regulation. In the present studies, we investigated the role of Efnb1 in vascular smooth muscle cell (VSMC) contractility and BP regulation. We revealed that reverse signaling through Efnb1 led to a reduction of RhoA activation and VSMC contractility *in vitro*. Consistent with this finding, *ex vivo*, there was an increase of RhoA activity accompanied by augmented myosin light chain phosphorylation in mesenteric arteries from mice with smooth muscle-specific conditional *Efnb1* gene knock-out (KO). Small interfering RNA knockdown of Grip1, a molecule associated with the Efnb1 intracellular tail, partially eliminated the effect of Efnb1 on VSMC contractility and myosin light chain phosphorylation. In support of these *in vitro* and *ex vivo* results, *Efnb1* KO mice on a high salt diet showed a statistically significant heightened increment of BP at multiple time points during stress compared with wild type littermates. Our results demonstrate that Efnb1 is a previously unknown negative regulator of VSMC contractility and BP and that it exerts such effects via reverse signaling through Grip1.

Eph kinases form the largest family of receptor tyrosine kinases. Eph kinases can be divided into A and B families based on their sequence homology (1). There are nine members in the Epha family and six members in the Ephb family. Each species does not necessarily have all the members of each family. In mice, there are only five members in the Ephb family. The ligands of Eph kinases are also cell surface proteins (2–4) and this dictates that interactions between Ephs and ephrins (Efns)[4] are mainly local and restricted to neighboring cells. Efns are divided into A and B families: the former are glycosylphosphatidylinositol-anchored cell surface proteins, and the latter are transmembrane proteins (2–4). Ephs and Efns interact promiscuously, but Ephas predominantly bind to Efnas, and Ephbs mainly bind to Efnbs (2–4). Interestingly, Efnbs may also transduce signals into cells upon binding to Ephbs, and this phenomenon is called reverse signaling (2–4).

The functions of Eph/Efn molecules in the central nervous system were the first to be studied in depth (3, 4). In recent years, their functions have been revealed in various other tissue and organs. These molecules are involved in immune regulation (5), intestinal and urorectal tract development and function (6, 7), angiogenesis (8), bone formation (9, 10), insulin secretion by islet β-cells (11), kidney glomerular filtration (12), and ionic homeostasis of vestibular endolymph fluid in the inner ear (13) to name a few.

There are a few reports showing that Efnb2 and Efna1 are expressed in vascular smooth muscle cells (VSMCs) (14–16), and VSMCs with Efnb2 deletion manifest compromised migration (14). One study has shown that Efna1 could trigger Epha4 signaling and actin stress fiber assembly (17). However, there

* This work was supported in part by Canadian Institutes of Health Research Grants MOP57697, MOP69089, and PPP85159 (to J. W.), IMH 79565 and MOP97829 (to H. L.), and MOP14496 (to E. T.); a Canadian Institutes of Health Research grant (to J. T.); grants from the Heart and Stroke Foundation of Quebec, the Quebec Ministry of Economic Development, Innovation and Export Trade (Grant PSR-SIIRI-069), and the J.-Louis Lévesque Foundation (to J. W.); and a group grant from the Fonds de la recherche en santé du Québec for Transfusional and Hemovigilance Medical Research (to J. W.).

[1] Both authors contributed equally to this work.

[2] Supported in part by Zhejiang Provincial Natural Science Foundation of China Grant Y2080374 and National Natural Sciences Foundation of China Project for Young Scientists 30800999.

[3] To whom correspondence should be addressed: CRCHUM, Notre-Dame Hospital, DeSève Pavilion, Rm. Y-5616, 1560 Sherbrooke St. E., Montreal, Quebec H2L 4M1, Canada. Tel.: 514-890-8000 (ext. 25164); Fax: 514-412-7596; E-mail: jianping.wu@umontreal.ca.

[4] The abbreviations used are: Efn, ephrin; BP, blood pressure; qPCR, real time quantitative polymerase chain reaction; VSMC, vascular smooth muscle cell; MLC, myosin light chain; HBSS, Hanks' balanced salt solution; Ab, antibody; AngII, angiotensin II; TRITC, tetramethylrhodamine isothiocyanate; PE, phenylephrine; HR, heart rate; SP, systolic pressure; DP, diastolic pressure; MAP, mean arterial pressure; SMC, smooth muscle cell; AT1R, AngII type I receptor; AR, adrenoreceptor; SH2, Src homology 2; GDI, GDP dissociation inhibitor; GEF, GDP exchange factor.

TABLE 1
qPCR primer sequences for β-actin, Efnb1, Grip1, Disheveled, and PDZ-RGS3 mRNA quantification

Gene	qPCR sequence product		PCR
	sense sequence	antisense sequence	
β-actin	5' -TCGTACCACAGGCATTGTGATGGA-3'	5' -TGATGTCACGCACGATTTCCCTCT-3'	200bp
Efnb1	5' -ACCAGGAAATCCGCTTCACCATCA-3'	5' -ACAGCATTTGGATCTTGCCCAACC-3'	199bp
Disheveled	5'-TCTCGGCTAGTTCGGAAGCACAAA-3'	5'-TGATGTTCAGGGACATGGTGGAGT-3'	112bp
Grip1	5'-ACAAGTCCCGTCCGGTTGTGATAA-3'	5'-TCTATCAGCAGCGTGGCTTCTTGT-3'	181bp
PDZ-RGS3	5'-TGGCAACAGGAGGAACAGTGGTAT-3'	5'-ATGTCTTCCAGCAGGAATGGGTCA-3'	170bp

are no studies to date on the function of Ephs and Efns in VSMC contractility and blood pressure (BP) regulation.

In an unrelated project, our DNA microarray assay showed that some genes controlling BP were differentially expressed in Ephb6 gene knock-out (KO) *versus* wild type (WT) thymocytes. This prompted us to investigate the roles of Ephs and Efns in BP regulation. In this report, we have demonstrated for the first time that Efnb1 regulates VSMC contractility and blood pressure in mice with conditional deletion of the *Efnb1* gene.

MATERIALS AND METHODS

Generation of Smooth Muscle Cell-specific Efnb1 KO Mice—The scheme, procedures, and verification of the generation of *Efnb1* floxed mice have been reported recently by us (18). *Efnb1* is an X-linked gene. Mice with loxP sites flanked by the first *Efnb1* exon were named $Efnb1^{f/f}$ (loxP insertions in both alleles in females) or $Efnb1^{f}$ (loxP insertion in one allele in males). They were backcrossed with C57BL/6 for five or 10 generations and then mated with smooth muscle myosin heavy chain promoter-driven *Cre* transgenic mice in the C57BL/6 background (smMHC-Cre-IRES-eGFP; Ref. 19) to obtain smooth muscle cell-specific *Efnb1* gene KO mice.

Reverse Transcription-Real Time Quantitative Polymerase Chain Reaction (RT-qPCR)—Efnb1, Grip1, Disheveled, and PDZ-RGS3 mRNA levels were measured by RT-qPCR. Forward and reverse primers and the size of amplified fragments are listed in Table 1. Total RNA from VSMCs or spleen cells was extracted using TRIzol® (Invitrogen) and then reverse transcribed with Superscript II™ reverse transcriptase (Invitrogen). The PCR condition for the reactions were as follows: 2 min at 50 °C and then 2 min at 95 °C followed by 45 cycles of 10 s at 94 °C, 20 s at 58 °C, and 20 s at 72 °C. β-Actin mRNA levels were used as internal controls, and data were expressed as signal ratios of test gene mRNA/β-actin mRNA.

Immunoblotting—The aorta and mesenteric arteries of WT and KO mice were isolated, washed twice with HBSS buffer, and then frozen in liquid nitrogen until use. The vessels were homogenized for 1 min at room temperature in 0.4 ml of radioimmunoprecipitation assay buffer, which contained PhosSTOP and protease inhibitor mixture (Roche Applied Science). The samples were spun at 12,000 rpm for 15 min at 4 °C, and the supernatants were collected. Twenty micrograms of proteins per sample were resolved by 12% SDS-PAGE. Proteins from the gel were transferred to PVDF membranes (Invitrogen), which were incubated in blocking buffer containing 5% (w/v) skimmed milk (for myosin light chain (MLC), 5% BSA was used in the blocking buffer) for 1 h at room temperature and then hybridized overnight at 4 °C with goat anti-mouse Efnb1 Ab (R&D Systems, Minneapolis, MN), rabbit anti-mouse β-actin Ab, mouse anti-mouse phospho-MLC mAb, or rabbit anti-mouse total MLC Ab (all from Cell Signaling Technology, Danvers, MA). The Abs were used at the manufactures' recommended dilutions or at 1:1000. The membranes were washed three times and incubated with corresponding second Abs, *i.e.* horseradish peroxidase-conjugated donkey anti-rabbit IgG Ab (GE Healthcare), horseradish peroxidase-conjugated sheep anti-mouse IgG Ab (GE Healthcare), or horseradish peroxidase-conjugated rabbit anti-goat IgG Ab (R&D Systems), for 90 min. The signals were detected with SuperSignal West Pico Chemiluminescent Substrate (Thermo Scientific, Rockford, IL).

VSMC Isolation—Mouse VSMC isolation was conducted as described by Golovina and Blaustein (20) with modifications. Briefly, the mesenteric arteries, including their secondary branches from the 10–15-week-old mice, were cleaned of the adventitia with fine forceps and sterile cotton-tipped applicators under sterile conditions. The isolated blood vessels were cut into small pieces (1 mm^3) and digested at 37 °C for 20 min in low Ca^{2+} HBSS containing both collagenase type II (347 units/ml, Worthington) and elastase type IV (6 units/ml) (Sigma-Aldrich). The digestion mixture was centrifuged at 1,500 × *g* for 5 min to bring down cells. The dissociated cells were suspended and plated on 12-well plates. The cells were cultured at 37 °C in Dulbecco's modified Eagle's medium (Wisent, St. Bruno, Quebec, Canada) supplemented with 15% fetal bovine serum (FBS) for 4–5 days before experimentation.

Immunofluorescence Microscopy—VSMCs were cultured in 24-well plates with a cover glass placed at the bottom of the wells. After 4–5 days, the cells were washed twice with PBS and fixed with paraformaldehyde (4%) for 20 min. For cell surface antigen staining, cells were blocked with 10% goat IgG in PBS for 20 min and then incubated with first Abs (2 μg/ml) goat anti-mouse Efnb1 Ab (R&D Systems), rabbit anti-mouse type 1a α adrenoreceptor Ab (Abcam Inc., Cambridge, MA), and rabbit anti-mouse angiotensin II (AngII) receptor Ia Ab (Santa Cruz Biotechnology, Santa Cruz, CA) overnight at 4 °C. Cells were then incubated with the corresponding second Abs (*i.e.* rhodamine-conjugated donkey anti-goat Ab (0.15 μg/ml; Jackson ImmunoResearch Laboratories, West Grove, PA) and FITC-conjugated sheep anti-rabbit IgG (0.2 μg/ml; Chemicon International, Billerica, MA)) overnight at 4 °C. For intracellular antigen staining, the cells were permeabilized with permeabilization buffer (BD Biosciences) for 20 min at 4 °C and then incubated with first Abs mouse anti-human α-actin mAb (2 μg/ml; Santa Cruz Biotechnology), rabbit anti-mouse MLC (2

TABLE 2
siRNA sequences of Grip1, Disheveled, PDZ-RGS3, and control siRNA

Gene	sets of siRNA sequence	
	sense sequence	antisense sequence
Disheveled	5'-rGrCrUrArGrUrUrCrGrGrArArGrCrArCrArArArUrGrCrCGT-3'	5'-rArCrGrGrCrArUrUrUrGrUrGrCrUrUrCrCrGrArArCrUrArGrCrCrG-3'
	5'-rArCrArGrCrUrCrArArGrUrArUrCrUrArUrArGrArGrUrCTT-3'	5'-rArArGrArCrUrCrUrArUrArGrArUrArCrUrUrGrArGrCrUrGrUrArC-3'
	5'-rCrGrCrCrUrArCrArArArUrUrCrUrUrCrUrUrCrArArGrUCC-3'	5'-rGrGrArCrUrUrGrArArGrArArGrArArUrUrUrGrUrArGrGrCrGrUrG-3'
Grip1	5'-rArGrArUrArArCrUrCrArGrArCrGrArGrCrArArGrArGrAGT-3'	5'-rArCrUrCrUrCrUrUrGrCrUrCrGrUrCrUrGrArGrUrUrArUrCrUrUrC-3'
	5'-rArGrCrGrUrGrGrArArCrUrUrGrGrArArUrArArCrCrArUCA-3'	5'-rUrGrArUrGrGrUrUrArUrUrCrCrArArGrUrUrCrCrArCrGrCrUrGrU-3'
	5'-rArCrArCrUrArGrArArArArUrCrGrArGrUrUrUrGrArUrGrUTG-3'	5'-rCrArArCrArUrCrArArArCrUrCrGrArUrUrUrCrUrArGrUrGrUrGrA-3'
RGS3	5'-rGrGrGrArArGrArGrArArCrArCrCrArArArUrArArArUrCrAAC-3'	5'-rGrUrUrGrArUrUrUrArUrUrUrGrGrUrGrUrUrCrUrCrUrCrCrCrUrG-3'
	5'-rGrCrCrArCrCrArUrArArArUrCrArCrGrCrUrArArGrArArGCA-3'	5'-rUrGrCrUrUrCrUrUrArGrCrGrUrGrArUrUrUrArUrGrUrGrGrCrArG-3'
	5'-rCrCrUrArCrArGrArGrArGrGrArArGrArArArCrUrUrCrACC-3'	5'-rGrGrUrGrArArGrUrUrUrCrUrUrCrCrUrCrUrCrUrGrUrArGrGrUrG-3'
Control	5' -rCrUrUrCrCrUrCrUrCrUrUrUrCrUrCrUrCrCrCrUrUrGrUGA-3'	5' -rUrCrArCrCrArArGrGrGrArGrArGrArArArGrArGrArGrGrArArGrGrA-3'

μg/ml; Santa Cruz Biotechnology), and rabbit anti-mouse phospho-MLC Ab (0.2 μg/ml; Santa Cruz Biotechnology) overnight at 4 °C. Cells were then washed and incubated with the second Abs rhodamine (TRITC)-conjugated AffiniPure $F(ab')_2$ fragment of goat anti-mouse IgG (heavy + light chain) (0.2 μg/ml; Jackson ImmunoResearch Laboratories), FITC-conjugated goat anti-mouse IgG (0.2 μg/ml; Bethyl Laboratories, Montgomery, TX), and FITC-conjugated sheep anti-rabbit IgG (0.2 μg/ml; Chemicon International), respectively, at room temperature for 2 h and imbedded with ProLong® Gold antifade reagent (Invitrogen). The stained cells were examined under a Zeiss microscope. In some experiments, the total fluorescence intensity of a cell and the cell size were measured using AxioVision software from Zeiss; results are presented as fluorescence intensity per arbitrary unit of cell area (1 pixel).

Measurement of VSMC Contractility—Cultured primary VMSCs were washed once with Ca^{2+}-free HBSS and cultured in the same solution. The cells were placed under a Zeiss microscope with environmental controls (37 °C and 5% CO_2). The cells were stimulated with phenylephrine (PE) (20 μM) or AngII (10 μM) (both from Sigma-Aldrich). These concentrations were determined to be optimal according to pilot studies. The cells were photographed continuously for 15 min at a rate of one picture per min. Fifteen or more cells were randomly selected, and their length was measured at each time point with Zeiss AxioVision software. The percentage of contraction was calculated as follows: percent contraction = (cell length at time 0 − cell length at time *x*)/cell length at time 0.

Measurement of Ca^{2+} Flux—VMSCs were incubated in 2% FBS, DMEM containing 5 μM Fura-2-AM for 30 min. The cells were washed in warmed medium for 15–20 min to remove extracellular dye. The cells were recultured in HBSS with Ca^{2+} (1.26 mM) and placed under a Zeiss microscope with environmental controls (37 °C and 5% CO_2). The cells were stimulated with PE (20 μM) and imaged for 5 min at a rate of six pictures per min. The excitation wavelengths were switched between 340 and 380 nm with an illumination time of 180 ms, and the emission wavelength was 510 nm. Signals from more than 15 randomly selected cells were registered, and the results are expressed as ratios of fluorescence intensity at 510 nm excited by 340 *versus* 380 nm.

Small Interfering RNA (siRNA) Transfection—siRNA of Grip1, Disheveled, and PDZ-RGS3 and negative control siRNA were synthesized by Integrated DNA Technologies (Coralville, IA); the sequences of these siRNAs are shown in Table 2. VSMCs were cultured for 4- 5 days with the last 16 h free of antibiotics and then transfected with a mixture of three pairs of siRNAs of a particular gene (each pair at a final concentration of 10 nM) using FuGENE HD X-tremeGENE siRNA Transfection Reagent (Roche Applied Science). The transfected VSMCs were further cultured for 24–36 h. Contractility was measured upon PE stimulation, and MLC phosphorylation was measured by immunofluorescence.

Transient Grip1 Overexpression in VSMCs—A Grip1 expression plasmid, pCEP4-Grip1, was constructed by cloning mouse *Grip1* cDNA (a NotI/HincII fragment of clone MGC80644 containing *Grip1* cDNA from position 1 to 4064 according to GenBank™ accession number BC072632 sequence) in the NotI/XhoI sites downstream of the CMV promoter in a mammalian cell protein expression vector, pCEP4. WT VSMCs were cultured for 6 days and then transfected with pCEP4-Grip1 or the control empty vector pCEP4 using 0.2 μg of plasmid DNA mixed with FuGENE HD X-tremeGENE siRNA Transfection Reagent (Roche Applied Science) per well of VSMCs in 6-well plates. Cell contraction was conducted 24 h later.

Activated RhoA Assay—GTP-associated activated RhoA levels in mesenteric artery smooth muscles were determined using a G-LISK RhoA Activation Assay Biochem kit (Cytoskeleton Inc., Denver, CO) according to the manufacturer's instructions.

Ex Vivo Vessel Constriction—Vessel constriction was studied *ex vivo* as described previously (21). Mesenteric artery segments (2 mm in length) of third order branches (exterior diameter, 125–150 μm) were stripped off the endothelium and mounted on 20-μm tungsten wires in small vessel myographs, stretched to optimal tension, and maintained in physiological saline solution (130 mM NaCl, 4.7 mM KCl, 1.18 mM KH_2PO_4, 1.17 mM $MgSO_4$, 1.17 mM $NaHCO_3$, 1.6 mM $CaCl_2$, 0.023 mM EDTA, 10 mM glucose aerated with 12% O_2, 5% CO_2, 83% N_2, pH 7.4) at 37 °C. After a 40-min stabilization period, arterial segments were challenged with 40 mM KCl physiological saline solution (KCl was substituted for an equivalent concentration of NaCl). Single cumulative concentration-response curves to the α_1-adrenergic receptor agonist PE (1 nM to 100 μM; Sigma) were charted. At the end of the protocol, maximal tension (E_{max}) was determined by changing the physiological saline solution to a solution containing 127 mM KCl. The data are expressed as percentages of E_{max}. Student's *t* tests were performed to compare concentration-response curves.

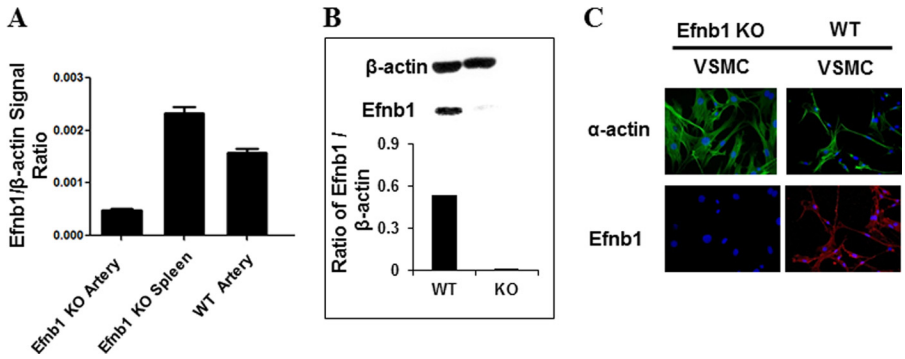

FIGURE 1. **Generation of mice with SMC-specific deletion of Efnb1.** *A*, deletion of Efnb1 at the mRNA level in the artery of male *Efnb1* KO mice. mRNA from the VSMCs and spleen cells of male *Efnb1* KO and WT mice was assessed for Efnb1 mRNA by RT-qPCR. Means ± S.D. of the ratios of Efnb1 *versus* β-actin signals are presented. *B*, deletion of Efnb1 at the protein level in Efnb1 KO arteries according to immunoblotting. Proteins extracted from the mesenteric arteries of *Efnb1* KO and WT mice were subjected to immunoblotting analysis. β-Actin levels were used as a loading control. The signal ratios of Efnb1 and β-actin (*lower panel*) were determined by densitometry. *C*, VSMC-specific deletion of Efnb1 protein in *Efnb1* KO mice according to immunofluorescence microscopy. VSMCs and non-VSMCs from *Efnb1* KO and WT mice were isolated from mesenteric arteries, and their Efnb1 (*red*; *lower row*) and α-actin (*green*; *upper row*) expression was detected by immunofluorescence microscopy. The experiments in this figure were repeated three times, and representative experiments are shown.

BP Measurements by Radiotelemetry—Mice were anesthetized with isoflurane and surgically implanted with TA11PA-C10 radiotelemetry sensors (Data Sciences International, St. Paul, MN) in the left carotid artery for direct measurement of arterial pressure and heart rate (HR) as described previously (22). Mice were given 7 days to recover. Next, BP and HR in conscious, freely moving mice were continuously recorded for 3 days using the Dataquest acquisition 3.1 system (Data Sciences International). Individual 10-s waveforms of systolic pressure (SP), diastolic pressure (DP), mean arterial pressure (MAP), and HR were sampled every 2 min throughout the monitoring period. To assess the impact of immobilization stress on BP and HR, BP and HR were measured continuously during 30-min immobilization in a restraining device (IITC Life Science, Woodland Hills, CA) (23). Raw data were processed by the Dataquest A.R.T Analysis program (24) and are presented as means ± S.E. The statistical significance of differences between the experimental groups was evaluated by unpaired *t* test and repeated measures analysis of variance tests with the StatView program. Values of $p < 0.05$ were considered to be statistically significant.

ELISA for Urine Catecholamine and Plasma AngII Measurements—The 24-h urine catecholamines were assayed using a catecholamine ELISA kit (Rocky Mountain Diagnostics, Colorado Springs, CO). The plasma AngII was measured using an angiotensin ELISA kit (Phoenix Pharmaceuticals, Burlingame, CA). The assays were conducted according to the manufacturers' instructions.

RESULTS

Generation of SMC-specific Efnb1 Conditional Gene KO Mice—Efnb1 null mutation causes embryonic lethality (25). To study the function of Efnb1 in VMSCs, we generated conditional KO mice (18). These mice (*Efnb1*$^{f/f}$ for females and *Efnb1*^{f} for males as *Efnb1* is an X-linked gene) were crossed with smMHC-*Cre*-IRES-*eGFP* transgenic mice (19). The resulting *Efnb1* conditional KO mice were named smMHC-*Cre-Efnb1*$^{f/f}$ for females and smMHC-*Cre-Efnb1*^{f} for males. For reasons to be elucidated, female smMHC-*Cre-Efnb1*$^{f/f}$ mice were embryonic lethal, and only male smMHC-*Cre-Efnb1*^{f} mice could be generated. Therefore, smMHC-*Cre-Efnb1*^{f} male mice (backcrossed to the C57BL/6 background for five or 10 generations) were used as KO mice throughout this study, whereas age-matched *Cre-Efnb1*^{f} male mice with the same generation of backcrossing were used as controls. These mice were called *Efnb1* KO and WT mice, respectively, hereafter.

As shown in Fig. 1*A*, the SMC-specific deletion of exon 1 in the genome resulted in Efnb1 mRNA deletion in *Efnb1* KO VSMCs but not in spleen cells of *Efnb1* KO mice according to RT-qPCR. The mRNA deletion in the KO arterial tissue was not complete probably because of the presence of small amounts of fibroblasts and endothelial cells in the vessel. Efnb1 deletion in KO VSMCs at the protein level was demonstrated by immunoblotting. As shown in Fig. 1*B*, Efnb1 could be detected from lysates of freshly isolated WT but not Efnb1 KO arteries.

Efnb1 deletion in VSMCs at the protein level was also clearly demonstrated by immunofluorescence (Fig. 1*C*) as WT α-actin-positive (*green*) VSMCs were Efnb1-positive (*red*), whereas α-actin-positive *Efnb1* KO VSMCs were Efnb1-negative. The result proved not only VSMC-specific deletion of Efnb1 in *Efnb1* KO mice but also the specificity of anti-Efnb1 Ab.

Efnb1 Engagement in VSMCs Results in Their Decreased Contractility Due to Efnb1 Reverse Signaling—We established a method of intravital microscopy to assess the contractility of KO and WT VSMCs. Isolated VSMCs were cultured for 4–5 days and then stimulated with vasoconstricting agents such as PE and AngII. Images of the cells were recorded for 15 min, and VSMC length was measured digitally at different time points. As illustrated in Fig. 2*A*, the majority of the cells (more than 80%) showed drastic contraction upon PE stimulation, and the contraction reached its maximum 15 min after the stimulation. This result indicates that after 4–5 days of culture the isolated VSMCs retained their contractile phenotype. A few non-contracting cells were likely contaminating fibroblasts. By randomly selecting contracting cells and measuring their length at different time points, we were able to assess their contractility as a function of cell length and time elapsed.

The contractility of *Efnb1* KO and WT VSMCs was measured on the basis of their responses to PE and AngII, but

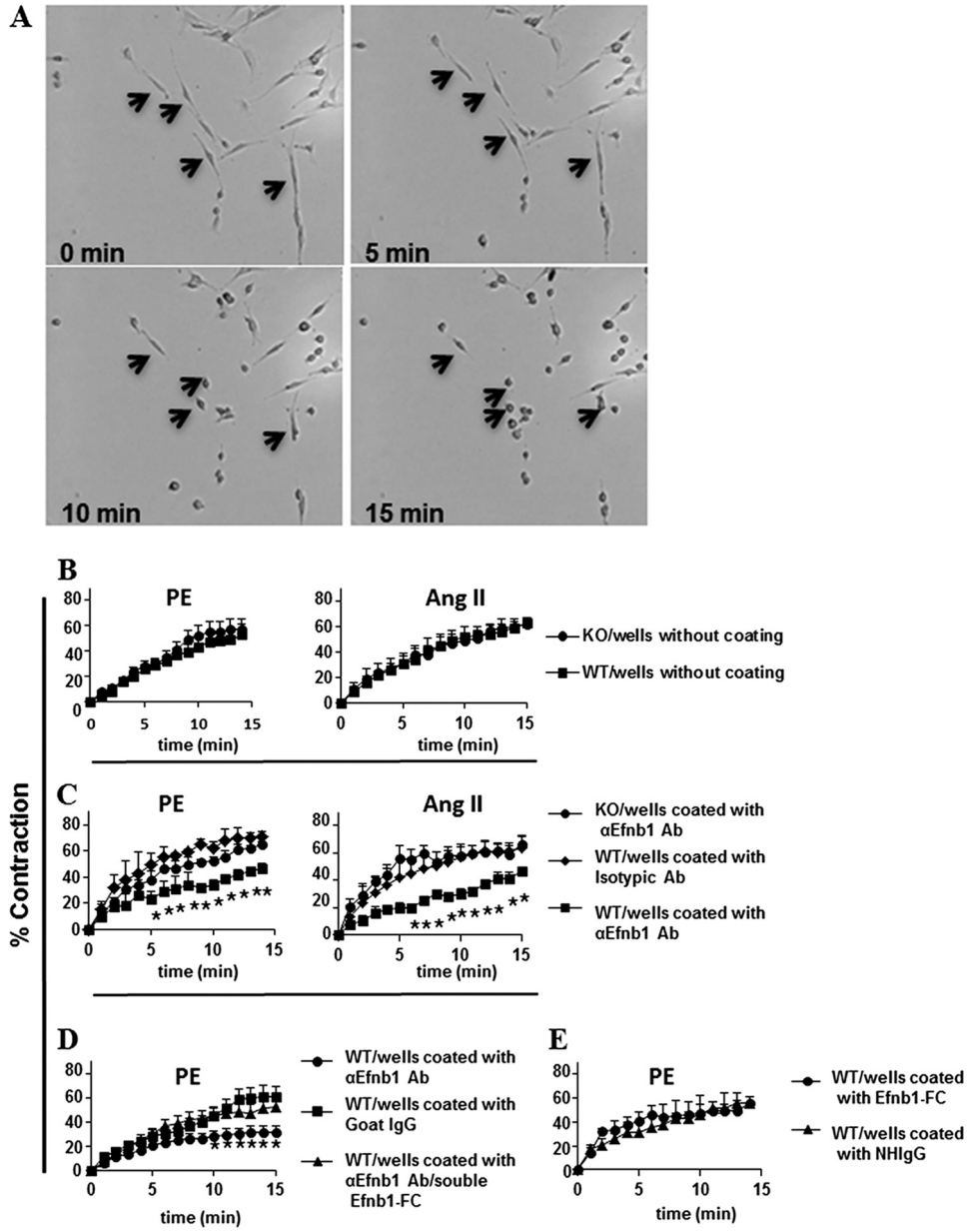

FIGURE 2. **Decreased contractility of Efnb1-engaged VSMCs.** *A*, VSMC contraction after PE stimulation. VSMCs were isolated from the mesenteric arteries of WT mice and cultured for 4 days. The cells were stimulated with 20 μM PE and imaged every min. Images at 0, 5, 10, and 15 min are shown. Four *arrows* point to the same four cells during the 15-min imaging period and show their contraction. The photographs also reveal that about 85% of the cells are capable of contraction, indicating the purity of VSMCs in such cell preparations. *B*, VSMCs from Efnb1 KO and WT mice presented similar contractility upon PE and AngII stimulation when cultured in uncoated wells. VSMCs from Efnb1 KO and WT mice were stimulated with 20 μM PE (*left column*) or 10 μM AngII (*right column*). The means $\pm$ S.D. of their percentage of contraction are illustrated. Data were analyzed with a paired Student's *t* test, but no significant difference was found. *C*, solid phase anti-Efnb1 Ab caused decreased contractility in WT but not *Efnb1* KO VSMCs. *Efnb1* KO or WT VSMCs were cultured in wells coated with goat anti-Efnb1 Ab (*αEfnb1 Ab*) or goat IgG-coated wells (2 μg/ml/well for 12-well plates during coating at 4 °C overnight) for 4 days and then stimulated with PE (20 μM; *left panel*) or AngII (10 μM; *right panel*). Means $\pm$ S.D. of percentage of contraction of these VSMCs are illustrated. *, significant differences between Efnb1 KO and WT VSMCs on anti-Efnb1 Ab-coated wells and between WT VSMCs cultured on isotypic Ab-coated wells and WT VSMCs cultured on wells coated with anti-Efnb1 Ab ($p < 0.05$; paired Student's *t* test). No significant difference was found between *Efnb1* KO VSMCs on anti-Efnb1 Ab-coated wells and WT VSMCs on isotypic Ab-coated wells. *D*, soluble recombinant Efnb1-Fc blocked the effect of solid phase anti-Efnb1 Ab on WT VSMC contraction upon PE stimulation. WT VSMCs were cultured in anti-Efnb1 Ab-coated wells in the presence of soluble Efnb1-Fc or normal human IgG (*NHIgG*) (both at 10 μg/ml). Means $\pm$ S.D. of percentage of contraction of these VSMCs stimulated with PE (20 μM) are illustrated. *, significant differences ($p < 0.05$; paired Student's *t* test). *E*, solid phase Efnb1-Fc had no effect on VSMC contraction stimulated by PE. WT VSMCs were cultured in Efnb1-Fc- or normal human IgG-coated wells (both at 10 μg/ml for coating). Percentage of contraction of these VSMCs stimulated with PE (20 μM) are illustrated. Data were analyzed with a paired Student's *t* test, but no significant difference was found. All experiments in this figure were conducted more than twice, and data from representative experiments are shown.

both types of VSMCs presented similar contractility (Fig. 2*B*). A possible explanation is that unlike VSMCs *in vivo* where the cells have close contact with neighboring VSMCs, allowing constant Eph/Efn engagement, the cultured VSMCs had limited interaction with neighboring cells and hence limited engagement between Efn and Eph especially in our culture conditions in which VSMCs were always non-confluent. Under such circumstances, the difference of Efnb1 KO and WT in contractility (if there was any) was difficult to detect.

We reasoned that if VSMCs were cultured on wells coated with anti-Efnb1 or recombinant Efnb1 then they might receive sufficient reverse or forward signaling, respectively, to mimic the *in vivo* condition. Indeed, when cultured in wells coated with anti-Efnb1 Ab and upon PE or AngII stimulation, WT VSMC contraction was reduced about 45–70% ((percentage of contraction of WT cells in isotypic Ab-coated wells)/(percentage of contraction of WT cells in anti-Efnb1 Ab-coated wells)) at multiple time points compared with those cultured in wells coated with isotypic control Ab (Fig. 2*C*). For Efnb1 KO VSMCs cultured in wells coated with anti-Efnb1 Ab, their contractility upon PE and AngII stimulation showed no significant difference from that of WT VSMCs cultured in wells coated with isotypic Ab. This is logical as anti-Efnb1 Ab could not react to these cells due to their null mutation of Efnb1. These results indicate that the function of Efnb1 in VSMCs is to dampen their contractility through reverse signaling. As the presence of solid phase anti-Efnb1 Ab dampened the contractility of WT VSMCs in response to both PE and AngII, the reverse signaling through Efnb1 was not specific to adrenoreceptor (AR) or AngII type I receptor (AT1R) but was probably on a downstream event after AR and AT1R signaling converges. The effects of solid phase anti-Efnb1 Ab in reducing WT VSMC contractility could be brought back to a near-normal level (the contraction was only about 10% lower than that of the WT cells cultured in isotypic Ab-coated wells without soluble Efnb1-Fc) by soluble Efnb1-Fc (Fig. 2*D*), demonstrating the specificity of the interaction between anti-Efnb1Ab and Efnb1-Fc.

When WT VSMCs were cultured in wells coated with recombinant Efnb1-Fc, the contractility of the cells was no different from that of cells cultured in wells coated with normal human IgG (Fc in Efnb1-Fc is of human origin) (Fig. 2*E*). This proves that forward signaling from Efnb1 to its receptors in VSMCs is of no consequence in terms of VSMC contractility.

Normal Expression of AR and AT1R in Efnb1 KO VSMCs—The reduced contractility of WT VSMCs in the presence of Efnb1 engagement in response to PE and AngII could be due to modulation of AR or AT1R expression by Efnb1. We therefore assessed the expression levels of AR and AT1R on VSMCs by immunofluorescence microscopy. The staining was quantified using Zeiss AxioVision software by measuring the immunofluorescence intensity per arbitrary unit of cell surface area (1 pixel). *Efnb1* KO VSMCs were no different from WT VSMCs in their AR and AT1R expression when cultured in uncoated wells (Fig. 3*A*). Although Efnb1 WT VSMCs, when cultured in wells coated with anti-Efnb1 Ab, showed reduced contractility compared with KO VSMCs, their AR and AT1R expression levels did not change (Fig. 3*B*). In this experiment, WT VSMC Efnb1 was stimulated by solid phase anti-Efnb1 Ab, whereas KO VSMCs could not be stimulated by the Ab due to a lack of Efnb1. The results indicate that the presence or absence of Efnb1 engagement did not alter AR and AT1R expression.

Effect of Efnb1 Reverse Signaling on Calcium Flux of VSMC—Calcium flux is an essential early signaling event common to both PE and AngII stimulation in VSMCs that leads to their contraction. We investigated whether the deletion or engagement of Efnb1 in VSMCs led to an increased basal calcium level and/or amplitude of calcium flux, which could in turn lead to increased contractility. As shown in Fig. 3, *C* (cells cultured in wells coated with isotypic control Abs with no Ca^{2+} in the medium) and *D* (cells cultured in wells coated with anti-Efnb1 Ab with no Ca^{2+} in the medium), Efnb1 KO and control WT VSMCs showed no significant difference in basal and stimulated intracellular calcium levels upon PE (*left panel*) and AngII (*right panel*) stimulation. Note that in Fig. 3*D* WT VSMCs received stimulation from solid phase anti-Efnb1 Ab, whereas KO VSMCs could not because of their lack of Efnb1. In Fig. 3, *C* and *D*, the calcium influx seen in these cells was mobilized from intracellular Ca^{2+} storage in sarcoplasmic reticulum.

We next cultured Efnb1 KO and WT VSMCs in medium containing Ca^{2+} and stimulated them with PE. In this case, the source of increased intracellular calcium in VSMCs came from both extracellular culture medium and intracellular sarcoplasmic reticulum. WT and KO VSMCs in wells coated with isotypic control Ab (Fig. 3*E*, *left panel*) again showed similar basal Ca^{2+} levels and Ca^{2+} flux. In this case, even if Efnb1 in WT VSMCs received some stimulation from neighboring cells, whereas KO VSMCs did not, there was no difference in their Ca^{2+} levels. We then cultured WT and KO VSMCs in wells coated with anti-Efnb1 Ab in the presence of calcium in the culture medium. In this case again, WT could receive stimulation from solid phase anti-Efnb1 Ab, whereas KO VSMC cannot due to their Efnb1 deletion. However, their basal Ca^{2+} levels and Ca^{2+} flux showed no differences (Fig. 3*E*, *right panel*).

The results from this section indicate that Efnb1 null mutation or anti-Efnb1 Ab-triggered reverse signaling in VSMCs does not affect the function of Ca^{2+} ion channels related to Ca^{2+} mobilization from either intracellular or extracellular sources. Therefore, the reduced VSMC contractility upon Efnb1 reverse signaling is not due to abnormalities of the immediate early signaling event, Ca^{2+} flux.

Effect of Efnb1 Reverse Signaling on VSMC MLC Phosphorylation and RhoA Activation—Because there was no difference in basal and flux levels of calcium in VSMCs with or without Efnb1 signaling, we wondered whether Efnb1 reverse signaling altered the sensitivity of VSMCs to Ca^{2+}. We evaluated these cells for their MLC phosphorylation, which is the main mechanism regulating VSMC sensitivity to Ca^{2+} (26, 27). Levels of total MLC and phosphorylated MLC *ex vivo* in freshly isolated arteries (with adventitia and endothelium removed) were determined by immunoblotting. As shown in Fig. 4*A*, there was a significant increase in levels of constitutive MLC phosphorylation but not total MLC in Efnb1 KO vessels compared with those in WT vessels. We next assessed constitutive MLC phosphorylation in cultured VSMCs by immunofluorescence microscopy, which was used because the amount of proteins that could possibly be obtained from these cultured VSMCs was too small for immunoblotting. Consistent with the findings of immunoblotting in vessels *ex vivo*, WT VSMCs cultured in anti-Efnb1 Ab-coated wells showed reduced levels of constitutive MLC phosphorylation (Fig. 4*B*, *right panel*) but not total MLC (Fig. 4*B*, *left panel*) compared with those without anti-Efnb1 stimulation (cultured in wells coated with isotypic control Ab). These results suggest that Efnb1 reverse signaling dampens VSMC responsiveness to Ca^{2+} flux by reducing MLC phosphorylation. Consistent

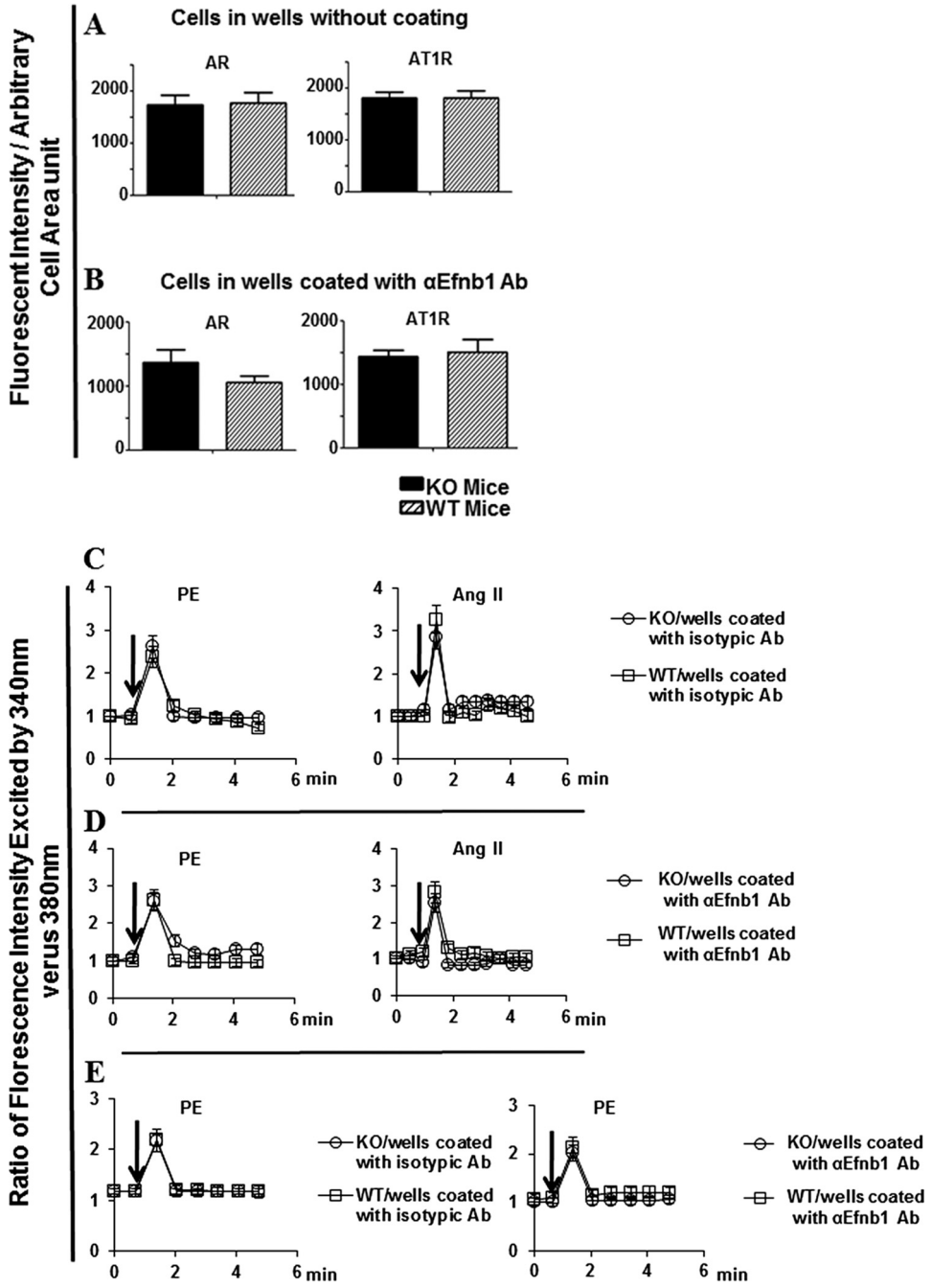

FIGURE 3. **Early Efnb1-mediated signaling events in VSMCs stimulated by PE and AngII.** *A*, normal AR and AT1R expression in *Efnb1* KO VSMCs. VSMCs from male *Efnb1* KO or WT mice were cultured in uncoated wells for 4 days and then stained with Abs against AR or AT1R as indicated. VSMCs were identified with anti-α-actin Ab staining. For each experiment, more than 15 α-actin-positive cells were randomly selected, and their total immunofluorescence intensity and cell size were registered. The means ± S.D. of the fluorescence intensity per arbitrary cell area unit (1 pixel) of all cells examined are shown. Data were analyzed with a paired Student's *t* test, but no significant difference was found. *B*, normal AR and AT1R expression in WT VSMCs with Efnb1 engagement. VSMCs from male WT mice were cultured in wells coated with goat anti-Efnb1 Ab (α*Efnb1Ab*) or normal goat IgG (2 μg/ml during coating) for 4 days, then stained with Abs against AR or AT1R, and analyzed as described above. Data were analyzed with a paired Student's *t* test, but no significant difference was found. *C–E*, normal Ca^{2+} flux in VSMCs with or without Efnb1 engagement. VSMCs from male *Efnb1* KO or WT mice were cultured for 4 days and then loaded with Fura-2 (5 μM). The cells were then placed in HBSS with or without 1.26 mM Ca^{2+} at 37 °C and stimulated with PE (20 μM) or AngII (10 μM). The ratio of emissions at 510 nm triggered by 340- *versus* 380-nm excitation in each cell was registered every 10 s for a duration of 5 min, and the means ± S.D. of the ratios of more than 15 randomly selected VSMCs are shown. The *arrows* indicate the time point at which PE was added. *C*, VSMCs from male *Efnb1* KO or WT mice were cultured in normal goat IgG-coated wells for 4 days and stimulated with PE (*left panel*) or AngII (*right panel*) in Ca^{2+}-free buffer. *D*, VSMCs from male *Efnb1* KO or WT mice were cultured in goat anti-Efnb1 Ab-coated wells and stimulated with PE (*left panel*) or AngII (*right panel*) in Ca^{2+}-free buffer. *E*, VSMCs from male *Efnb1* KO or WT mice were cultured in goat anti-Efnb1 Ab-coated or normal goat IgG-coated wells and stimulated with PE (*left panel*) or AngII (*fight panel*) in Ca^{2+}-containing buffer. All experiments in this figure were conducted more than twice, and data from representative experiments are shown.

findings between immunoblotting and quantitative immunofluorescence microscopy validated the microscopy as an alternative method to immunoblotting.

As activated RhoA could increase MLC phosphorylation via the RhoA-associated kinase/myosin phosphatase pathway (28), we wondered whether Efnb1 reverse signaling in VSMCs

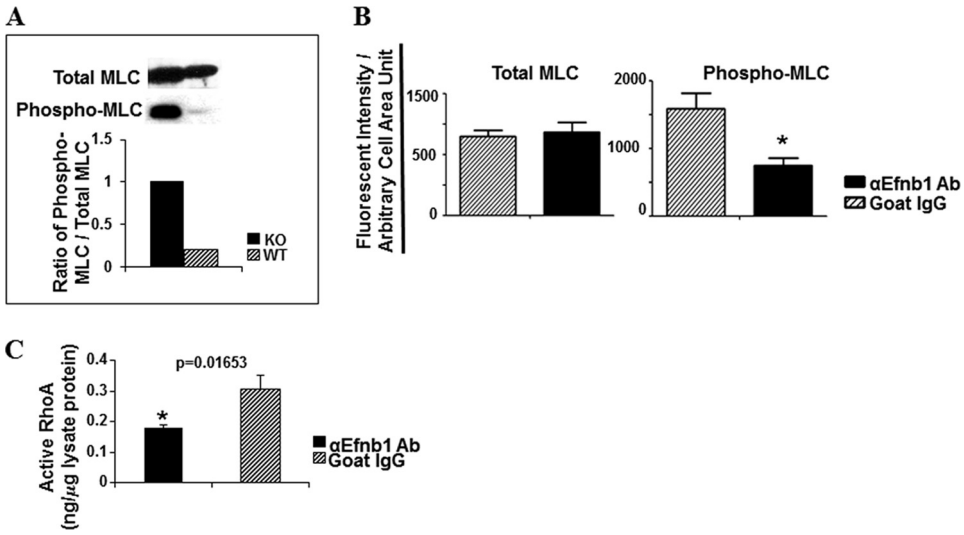

FIGURE 4. **MLC phosphorylation and RhoA activation in VSMC.** *A*, increased constitutive MLC phosphorylation in Efnb1 KO VSMCs *ex vivo*. The mesenteric arteries of Efnb1 KO and WT mice were cleared of adventitia and homogenized. The proteins of these tissues were analyzed for phosphorylated MLC (*Phospho-MLC*) and total MLC expression by immunoblotting as indicated. Densitometry was performed to quantify the signals, and the data are expressed as ratios of phosphorylated MLC *versus* total MLC signals (*bar graph*, *lower panel*). *B*, reduced MLC phosphorylation in Efnb1-engaged WT VSMCs. VSMCs from male WT mice were cultured in wells coated with goat anti-Efnb1 Ab (α*Efnb1Ab*) or normal goat IgG (2 μg/ml during coating) for 4 days. Total MLC (*left panel*) and phosphorylated MLC (*right panel*) of VSMCs were detected by immunofluorescence. The means ± S.D. of fluorescence intensity per arbitrary cell area unit of more than 15 randomly selected α-actin-positive cells examined are shown in the *bar graphs*. *, significant differences ($p < 0.05$; paired Student's *t* test). *C*, increased RhoA activation in Efnb1-engaged WT VSMCs. VSMCs from WT mice were cultured in wells coated with goat anti-Efnb1 Ab or normal goat IgG (2 μg/ml during coating) for 4 days. The cells were then harvested, and the GTP-associated RhoA in the cell lysates was determined in duplicate. The experiments were repeated twice, and the results are consistent. A representative set of data is shown. *, significant differences ($p < 0.05$; paired Student's *t* test).

resulted in RhoA activation. Indeed, when WT VSMCs were cultured in wells coated with anti-Efnb1 Ab, there was a significant increase in the GTP-bound RhoA level compared with cells cultured in wells coated with isotypic control Ab (normal goat IgG) (Fig. 4*C*).

Identification of Grip1 as Component in Efnb1 Reverse Signaling Pathway in Controlling VSMC Contraction—Because we discovered that reverse signaling is critical for the effect of Efnb1 on VSMC contraction, we attempted to identify components of the Efnb1 reverse signaling pathway. The intracellular tail of Efnb1 shows no direct biological activity, but it has three conserved tyrosine phosphorylation sites, which are known to interact with SH2 domain-containing adaptors such as Dishevelled (29). In addition, the C terminus of Efnb1 possesses a PDZ-binding domain (2), which could interact with PDZ-containing proteins such as Grip1 (30) or PDZ-RGS3 (31). To test the relevance of these adaptor proteins in mediating Efnb1 reverse signaling in VSMCs and its effect on VSMCs, we used siRNA to knock down the expression of Disheveled, Grip1, and PDZ-RGS3 in WT VSMCs. The expression and knockdown of these genes were confirmed at the mRNA level (Fig. 5*A*). When Efnb1-engaged WT VSMCs (*i.e.* VSMCs cultured in anti-Efnb1 Ab-coated wells), whose contractility was depressed about 40% at multiple time points compared with the controls, were transfected with Grip1 but not PDZ-RGS3 or Disheveled siRNA, they regained about 50% of their lost strength (Fig. 5*B*). On the other hand, Grip1 siRNA had no effect on VSMCs without Efnb1 engagement (VSMCs cultured in wells without anti-Efnb1 Ab coating; Fig. 5*C*). This shows that the effect of Grip1 siRNA is specific to Efnb1 reverse signaling but does not exert its effect via other pathways by itself. These results indicate that diminished Grip1 expression blocks the negative effect of Efnb1 engagement on VSMC contraction.

Conversely, when Grip1 was overexpressed in WT VSMCs without anti-Efnb1 stimulation, these cells showed about 50% reduced contractility, mimicking the effect of Efnb1 reverse signaling (Fig. 5*D*). These data demonstrate that Grip1 is a relevant adaptor protein that mediates Efnb1 reverse signaling in VSMCs to achieve reduced VSMC contractility.

We further demonstrated that Grip1 knockdown resulted in an increased level of MLC phosphorylation but not total MLC protein in Efnb1-engaged WT VSMCs (Fig. 5*E*); such an increase is likely a basis for the increased VSMC contractility that was caused by Grip1 siRNA transfection. This places Grip1 upstream of MLC phosphorylation in the Efnb1 reverse signaling pathway.

Ex Vivo Findings in Mesenteric Arteries from Efnb1 KO Mice—We wondered whether the reduced RhoA activation and contraction of cultured VSMCs upon Efnb1 activation were reflected in freshly isolated small arteries, which control vascular resistance and hence BP. GTP-associated RhoA levels in mesenteric arteries stripped of endothelium were first assessed. As shown in Fig. 6*A*, the arteries from the KO mice manifested significantly heightened GTP-associated RhoA levels compared with those from WT mice. This is consistent with the findings from anti-Efnb1 Ab-stimulated VSMCs, which had reduced RhoA activation.

However, *ex vivo* vessel constriction tests on freshly isolated mesenteric arteries from KO and WT mice did not reveal a significant difference with or without endothelium upon PE stimulation (Fig. 6*B*). Possible reasons for this observation are discussed later.

Efnb1 KO Mice Presented Higher Increments of BP than WT Mice during Immobilization Stress—The above findings regarding dampening VSMC contractility by Efnb1 engagement suggest that smooth muscle cell-specific *Efnb1* null muta-

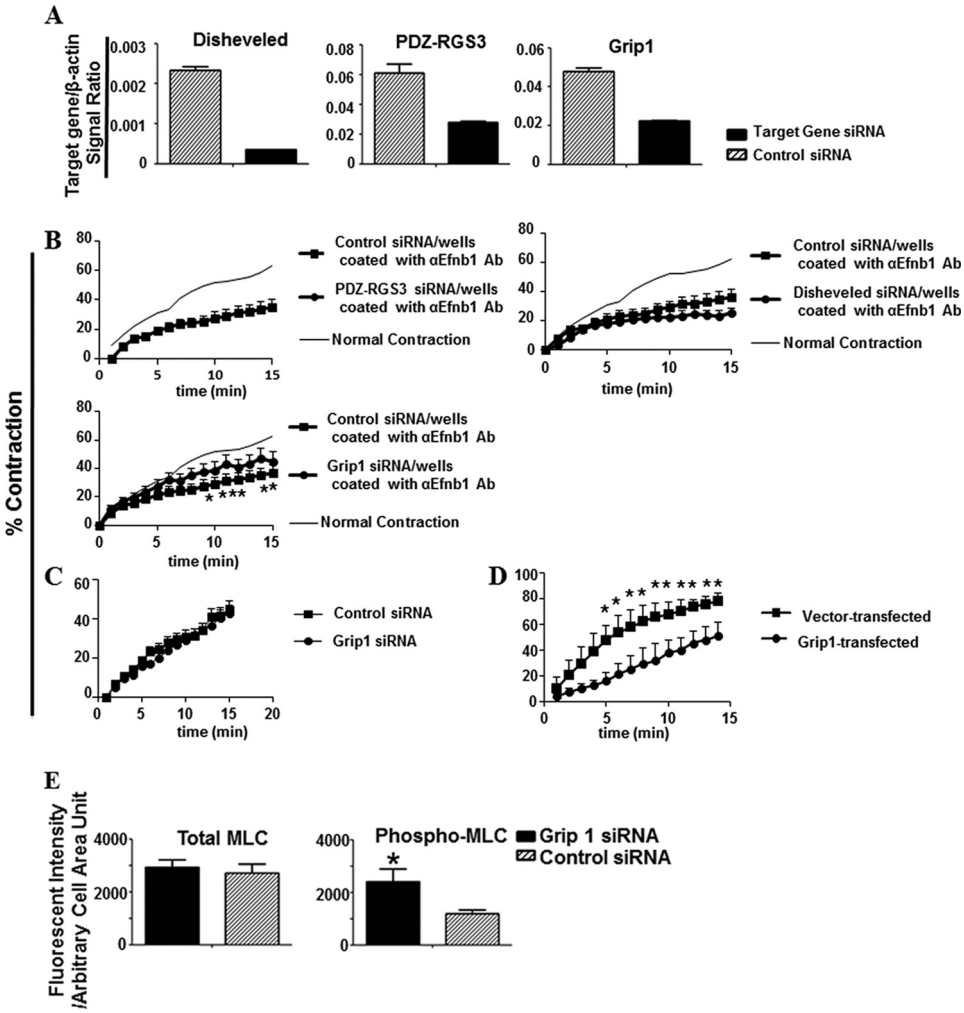

FIGURE 5. **Grip1 in Efnb1 reverse signaling pathway.** *A*, effective knockdown of Grip1, Disheveled, and PDZ-RGS3 mRNA by siRNA. VSMCs from WT mice were transfected with 30 nM siRNA targeting Grip1, Disheveled, or PDZ-RGS3 or with control siRNA. After an additional 4 h of culture, the mRNA levels of these three genes were measured by RT-qPCR, and the data are expressed as the means ± S.D. of signal ratios between the test genes and β-actin. *B*, Grip1 knockdown by siRNA partially reversed the inhibitory effect of solid phase anti-Efnb1 Ab. VSMCs from WT males were cultured in wells coated with goat anti-Efnb1 Ab (*αEfnb1 Ab*) (2 μg/ml for coating). After 2 days, the cells were transfected with 30 nM siRNA targeting Grip1, Disheveled, or PDZ-RGS3 or control siRNA. On day 4 of culture, the cells were stimulated with PE (20 μM), and their percentage of contraction was registered. Means ± S.D. of the percentage are shown. The *thin line* (indicated as *Normal Contraction*) represents the mean percentage of contraction of VSMCs cultured in wells coated with normal goat IgG (2 μg/ml) without siRNA transfection (for better visual effect, the S.D. of each time point in this control is omitted). *C*, the contractility of VSMCs cultured in uncoated wells is not affected by Grip1 siRNA. VSMCs from WT males were cultured in normal wells for 4 days and then transfected with Grip1 or control siRNA. Their contraction in response to 20 μM PE was measured. Means ± S.D. of the percentage are shown. No significant statistical difference was found (Student's *t* test) between VSMCs transfected with Grip1 or VSMCs transfected with control siRNA. *D*, Grip1 overexpression in VSMCs led to decreased contractility. WT VSMCs were cultured for 6 days and transfected with pCEP4-Grip1. Cell contraction stimulated by PE (20 μM) was conducted 24 h later, and means ± S.D. of percentage of contraction are shown. *E*, Grip1 knockdown by siRNA resulted in increased MLC phosphorylation (*Phospho-MLC*) in Efnb1-engaged WT VSMCs. VSMCs from WT males were cultured in wells coated with goat anti-Efnb1 Ab and transfected with Grip1 or control siRNA as described in *D*. The means ± S.D. of fluorescence intensity per arbitrary cell area unit of more than 15 cells are shown in the *bar graphs*. All experiments in this figure were conducted more than twice, and data from representative experiments are shown. *, significant differences ($p < 0.05$; paired Student's *t* test).

tion might augment BP. Thus, we measured the BP of male Efnb1 KO mice by telemetry. On a normal diet alone (Fig. 7*A*), on a normal diet under stress alone (data not shown), or on a high salt diet alone (Fig. 7*B*), Efnb1 mice and control WT mice presented no significant difference in their SP, DP, MAP, or HR. BP control has multiple compensatory mechanisms. A BP phenotype might be manifested only when the compensation is stretched to the limit. Indeed, the role of Efnb1 in BP regulation was revealed when the KO mice (average age, 21 weeks old) were in a condition that combined a high salt diet and immobilization stress. At several time points, *Efnb1* KO mice showed significantly higher increments of SP, DP, and MAP (ΔSP, ΔDP, and ΔMAP, respectively; *i.e.* the BP during stress minus the BP of the resting status of the same animal) (Fig. 7*C*). Such increased ΔBP was a reproducible phenomenon. In a separate experiment carried out on 16-week-old mice, such a statistically significant phenotype was also observed even with a small sample size ($n = 3$) (Fig. 7*D*). This is the first time a role of any Efn molecules in BP control has been discovered.

We also observed (Fig. 7*C*) that during stress on a high salt diet, Efnb1 KO mice had a significantly higher HR increment (ΔHR) than WT mice. Obviously, the higher ΔHR contributed to higher stress BP in these mice along with increased VSMC contractility as we have proven *in vitro*. The reason why *Efnb1* deletion heightened ΔHR in this particular experiment is not

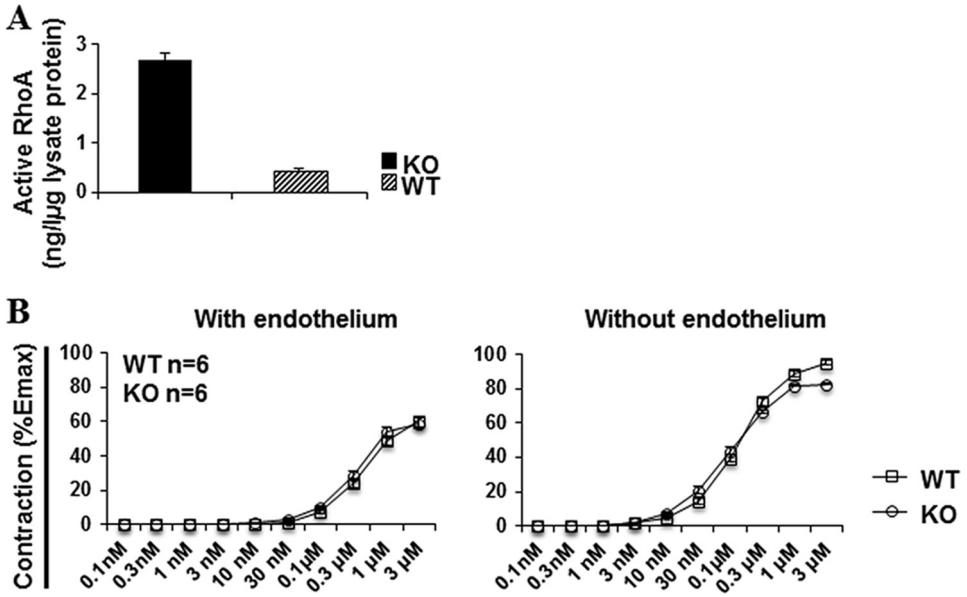

FIGURE 6. **GTP-associated RhoA expression and vasoconstriction of *Efnb1* KO mesenteric arteries.** *A*, activated RhoA in Efnb1 mesenteric arteries. The mesenteric arteries of *Efnb1* KO and WT mice were cleared of adventitia and homogenized. The proteins of these tissues were analyzed for GTP-associated RhoA levels in duplicate. The experiment was repeated twice, and data of a representative experiment are shown as mean ± S.D. of GTP-RhoA concentration per microgram of total protein. *, $p < 0.05$ according to paired Student's *t* test. *B*, contractility of mesenteric arteries from *Efnb1* KO and WT mice following PE stimulation. Segments (2 mm) of the third order branch of the mesenteric artery with endothelium or with endothelium removed were stimulated with PE. A single cumulative concentration-response curve to PE (1 nM to 100 μM) was obtained. The maximal tension (E_{max}) was determined by challenging the vessels with physiological saline containing 127 mM KCl. Vessel contractility is expressed as a percentage of the E_{max}. Data from three mice per group were pooled, and means ± S.E. are shown. There is no significant difference between KO and WT vessels (paired Student's *t* test).

clear and is under investigation, but the phenotype does not seem to be consistent and reproducible. As seen in Fig. 7*D*, in a similar experiment, such a heightened ΔHR increment was not present.

Normal Levels of Urinary Catecholamines and Plasma AngII of Efnb1 KO Mice—The *Efnb1* KO mice used in this study had conditional *Efnb1* KO in SMCs, and the phenotype of the mice was attributed to the deletion of Efnb1 in SMCs. To rule out the unlikely possibility that such conditional KO also affects the endocrine system, which in turn contributes to the enhanced VSMC contractility and stress BP, we assayed the 24-h urine catecholamines right after stress or without stress (Fig. 8*A*) and plasma AngII (Fig. 8*B*) of *Efnb1* KO mice. The results showed no significant difference in these parameters between *Efnb1* KO and control WT mice, ruling out the possible effect of conditional *Efnb1* deletion on the secretion of these hormones.

DISCUSSION

We for the first time have discovered that Efnb1 is likely involved in BP control by regulating VSMC contractility. Efnb1 engagement in mouse VSMCs resulted in their decreased contractility *in vitro*, whereas *Efnb1* null deletion in smooth muscle cells heightened the increment of BP during stress in mice on a high salt diet *in vivo*. Such regulation depended on reverse signaling of Efnb1 into VSMCs, and this reverse signaling modulated the levels of GTP-associated RhoA and MLC phosphorylation in VSMCs. Grip1, an adaptor protein, was a component in the Efnb1 reverse signaling pathway, and it mediated the effect of Efnb1 on VSMC contractility and MLC phosphorylation. A few issues are discussed below.

Efnb1 is vital during embryonic development. Complete deletion of Efnb1 leads to lethality during the fetal stage (25). Although male Efnb1 KO mice could be obtained, their occurrence was below the rate expected according to Mendel's law. It is known that *LoxP-Cre*-mediated deletion is not an all or none event, and there is variation in Cre expression even with the same copy number of *Cre* genes in the transgenic genome (32). Leaky transgenic Cre expression outside the targeted tissue is also frequently encountered. We speculate that fetuses with stronger Cre expression might become embryonic lethal due to either a higher degree of Efnb1 deletion in SMCs or leaky Cre expression in other tissues. No female smMHC-*Cre-Efnb1*$^{f/f}$ mice were ever born. This might be a result of essential interaction between Efnb1 and certain molecule(s) whose necessity is different in male and female fetuses.

A change in the intracellular Ca^{2+} level in VSMCs is a common and early signaling event after AR and AngII receptor activation. We noticed that the increase in VSMC Ca^{2+} occurred within 1 min after PE stimulation, a time frame compatible with that under a physiological condition *in vivo* under which arteries will constrict quickly upon adrenaline stimulation. However, it took about 15 min for cultured VSMCs to achieve maximal contraction. This is because the cultured VSMCs adhere to the wells and need to master enough force to gradually dislodge themselves from the plastic well surface to complete the contraction, whereas VSMCs in the vessels are free standing and can contract without much hindrance.

The increased intracellular Ca^{2+} in VSMCs comes from the influx of Ca^{2+} from the extracellular milieu via L-type voltage-gated calcium channels on the plasma membrane but is mainly from the mobilization of a Ca^{2+} reserve in sarcoplasmic reticulum via ryanodine and inositol trisphosphate receptors on the sarcoplasmic reticulum membrane. The subsequent ebbing of

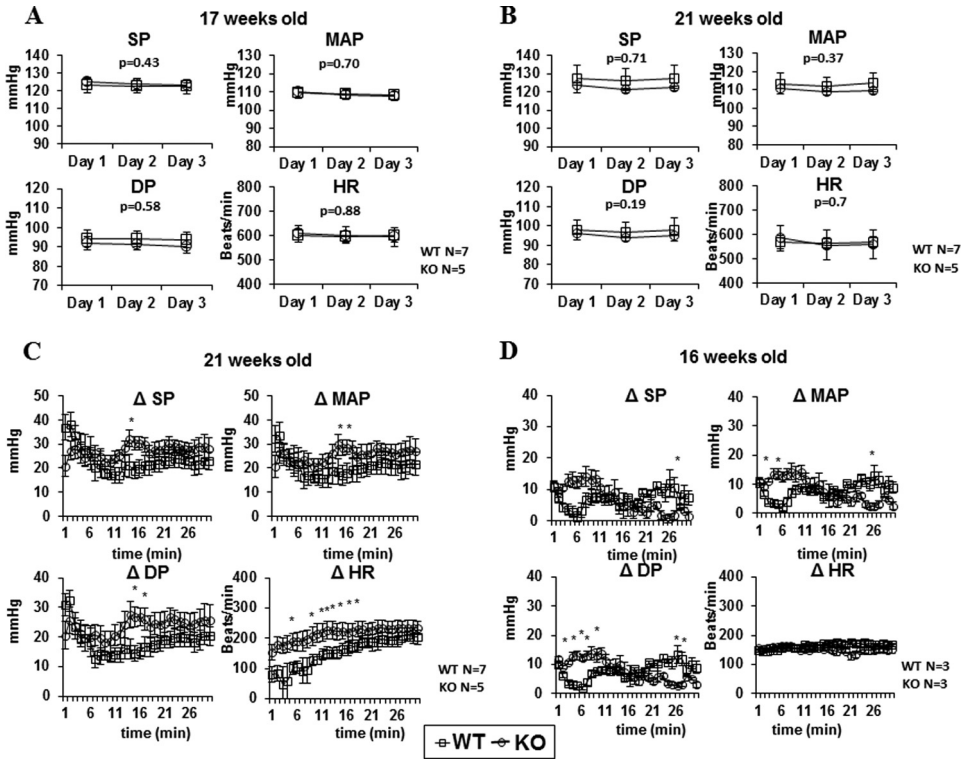

FIGURE 7. **Blood pressure and heart rate of *Efnb1* KO mice.** *A* and *B*, male *Efnb1* KO mice in the C57BL/6 background (F10) on a normal diet or high salt diet presented normal BP and HR. *A*, mice (17 weeks old) were on a normal diet. *B*, mice (21 weeks old) were on a high salt diet for 3 weeks. BP and HR were measured for 3 days by telemetry starting at least 7 days after transmitter implantation. For mice on a high salt diet, BP and HR were measured 3 weeks after the initiation of the high salt diet. The number per group is indicated. Values are expressed as mean 24-h BP and HR for each day ±S.E. *C*, male *Efnb1* KO mice (after 10 generations of backcrossing to the C57BL/6 background) on a high salt diet under immobilization stress presented an augmented increment of BP. SP, DP, MAP, and HR of 21-week-old male *Efnb1* KO and WT mice (the number per group is indicated) on a high salt diet for 3 weeks were recorded by telemetry during 30-min immobilization stress. The data are expressed as means ± S.E. of increments (Δ) of SP, DP, MAP, and HR. ΔSP, ΔDP, ΔMAP, and ΔHR were calculated as follows: Δ = value during stress − value during the resting period. *D*, male *Efnb1* KO mice (after five generations of backcrossing to the C57BL/6 background from the 129/sv × C57BL/6 background) on a high salt diet under immobilization stress presented an augmented increment of BP. SP, DP, MAP, and HR of 16-week-old male *Efnb1* KO and WT mice (the number per group is indicated) on a high salt diet for 3 weeks were recorded by telemetry during 30-min immobilization stress. ΔSP, ΔDP, ΔMAP, and ΔHR are shown. Data in this figure were analyzed by an unpaired *t* test and repeated measures analysis of variance, and the *p* values are shown. * indicates $p < 0.05$.

the intracellular Ca^{2+} depends on large conductance Ca^{2+}-activated K^+ channels on the plasma membrane and the sarcoendoplasmic reticulum Ca^{2+}-ATPase pump on the sarcoplasmic reticulum membrane (33, 34). VSMCs in the presence or absence of Efnb1 reverse signaling presented similar basal Ca^{2+} levels and Ca^{2+} flux after PE and AngII stimulation. This is also true regardless whether there is extracellular Ca^{2+} in the medium. This indicates that all the signaling components (*e.g.* AR, AngII receptor, L-type voltage-gated calcium channels, ryanodine receptors, inositol trisphosphate receptors, large conductance Ca^{2+}-activated K^+ channels, and sarcoendoplasmic reticulum Ca^{2+}-ATPase pumps) leading to Ca^{2+} flux are not modulated by Efnb1 reverse signaling.

In addition to the intracellular Ca^{2+} level, VSMC contractility is regulated by their sensitivity to Ca^{2+}, and the sensitivity is regulated by the degree of MLC phosphorylation (26, 27). We found that in the absence of Efnb1 the constitutive MLC phosphorylation in artery proteins was drastically augmented. The converse is also true: with Efnb1 engagement, VSMCs showed decreased MLC phosphorylation. Conceivably, such modulation of MLC phosphorylation leads to altered VSMC Ca^{2+} sensitivity and consequently altered VSMC contractility.

We have tried to identify components in the Efnb1 reverse signaling pathway that regulate MLC phosphorylation and VSMC contraction. We discovered that RhoA activation in the form of GTP-associated RhoA was reduced in anti-Efnb1 Ab-stimulated VSMCs. Compatible with such a finding, RhoA activation was augmented in the mesenteric artery smooth muscles of KO mice compared with that in WT mice. Activated RhoA can activate RhoA-associated kinase, which phosphorylates myosin phosphatase. The phosphorylation of the phosphatase reduces its activity, which then prolongs the phosphorylation of MLC (28). This might be a mechanism to increase the responsiveness of MLC to Ca^{2+} flux in the absence of Efnb1 reverse signaling.

An additional search of the components in the Efnb1 reverse signaling pathway identified Grip1 as its knockdown partially reverses the effect of Efnb1 on dampening VSMC contractility. Whether and how Grip1 is connected to RhoA activation, which will in turn promote MLC phosphorylation, is not clear, and we can only speculate at this point. Grip1 is an adapter protein containing seven PDZ domains (35), which can associate with the PDZ-binding domain at the C termini of Efnbs (28). It is possible that the remaining PDZ domains in Grip1 might interact with modulators of RhoA activity such as GDP dissociation inhibitors (GDI) or GDP exchange factors (GEF) and influence their functions, which will in turn regulate RhoA activity. Indeed, Grip1 can associate with a Rho-GDI (36) and a

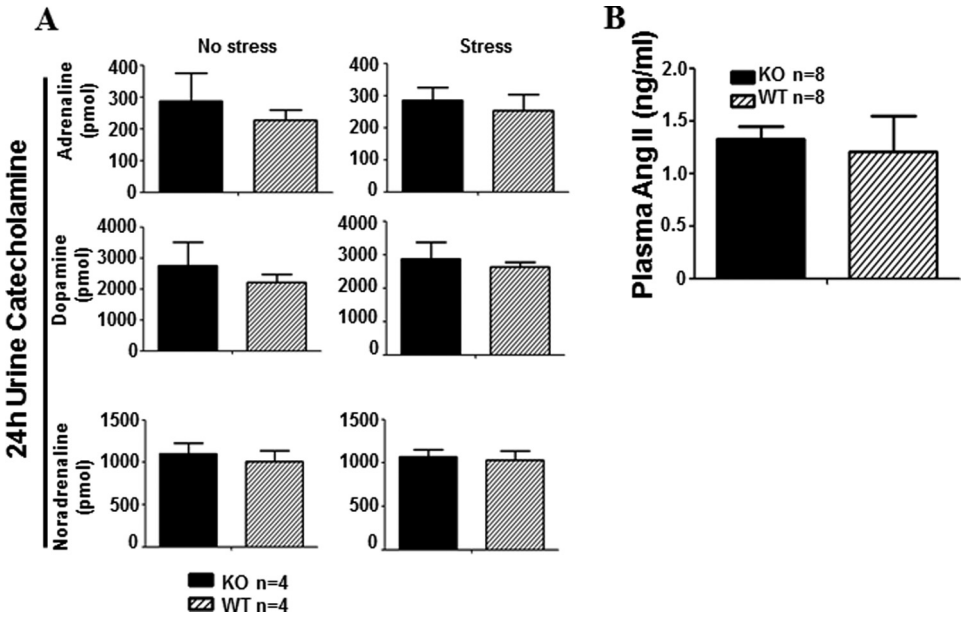

FIGURE 8. **Normal urine and plasma hormone levels in *Efnb1* KO and WT mice.** *A*, 24-h urine catecholamine levels after stress in male *Efnb1* KO mice. Male *Efnb1* KO and WT mice were placed in metabolic cages without prior stress or immediately after immobilization stress. Urine was collected during a 24-h fasting period. Urinary catecholamines were measured by ELISA. The number of mice per group and means ± S.D. of the hormones in 24-h urine are presented. No statistically significant difference was found (Student's *t* test) between KO and WT mice. *B*, plasma AngII levels in male *Efnb1* KO and WT mice. Plasma AngII of male *Efnb1* KO and WT mice was measured by ELISA. The number of mice per group and means ± S.D. of the hormone concentrations are shown. No statistically significant difference was found (Student's *t* test) between the KO and WT mice.

Ras-GEF (37) through its PDZ domains. Validation of such hypotheses is in progress.

Consistent with most of the *in vitro* and *ex vivo* findings, *Efnb1* KO mice manifested an augmented increment of SP, DP, and MAP during stress compared with WT mice when they were on a high salt diet. Although the increase was only statistically significant at several time points, this finding is genuine because it was reproducible in two independent experiments. BP, a vital physiological parameter, is tightly regulated by multiple compensatory mechanisms at the levels of vascular tone, blood volume, and cardiac output. It is not easy to override all these compensatory mechanisms to achieve an overt BP phenotype. Any molecule that could cause an overt BP phenotype (even a minimal one) has much more than a minimal role in BP regulation. This is especially true for Efnb1, which is a member of the Efnb subfamily. The Efnb subfamily has three Efnb members that have redundant functions and interact promiscuously with Ephs. Such redundancy might have further diminished the BP phenotype of *Efnb1* KO mice so that BP up-regulation in the KO mice is not manifested on a normal diet or under stress while on a normal diet but is only revealed with a combination of a high salt diet and stress. Under such conditions, the compensation mechanisms are finally overwhelmed. It is very likely that other Efnbs in addition to Efnb1 and some Ephb members are also involved in VSMC contractility and BP control. Our additional study showed that this is indeed the case: we have found that *Ephb6* KO mice have BP and VSMC contractility phenotypes similar to that of *Efnb1* KO mice (38).

There is some discrepancy among certain findings in our study. *Ex vivo*, RhoA activation and constitutive phosphorylation of MLC in the smooth muscle of the mesenteric arteries from KO mice were elevated. This is consistent with augmented BP in KO mice *in vivo* compared with WT mice when they were under stress and on a high salt diet. This is also compatible with the findings in cultured VSMCs in that VSMC contractility was reduced upon Efnb1 engagement. However, why did we not see increased *ex vivo* contraction of mesenteric arteries from KO mice compared with that from WT mice (Fig. 6*B*), and why could the lack of increased contraction in vessels translate into the *in vivo* phenotype of increased BP? It is possible that a subtle and minor increase of vasoconstriction is present in the vessel, but our vasoconstriction tests *ex vivo* are not sensitive enough to reveal it. Such an increase (as it is subtle and minor) was not revealed *in vivo* when mice were on a normal diet or in mice that had undergone immobilization stress alone. It only manifested itself when the KO mice were assaulted with both a high salt diet and immobilization stress, which overcome most of the compensation mechanisms in BP regulation.

Based on our findings, we speculate that under a physiological condition Efnb1 (or other Efnb members) on VSMCs interact(s) with Ephs in neighboring VSMCs or endothelial cells, and such interactions modulate VSMC contractility. Because the expression of Efnb1 (or other Efnb members) and its binding partner Ephs is unlikely to change instantly, the physiological role of Efnb1 (or other Efnbs) and Ephbs could be basal vascular tone regulation. These findings have enhanced our understandings of BP regulation mechanisms.

Acknowledgment—We sincerely thank Dr. Michael Kotlikoff for generously providing the smMHC-Cre-IRES-eGFP transgenic mice.

REFERENCES

1. Eph Nomenclature Committee (1997) Unified nomenclature for Eph family receptors and their ligands, the ephrins. *Cell* **90,** 403–404

2. Pasquale, E. B. (2008) Eph-ephrin bidirectional signaling in physiology and disease. *Cell* **133,** 38–52
3. Wilkinson, D. G. (2000) Eph receptors and ephrins: regulators of guidance and assembly. *Int. Rev. Cytol.* **196,** 177–244
4. Flanagan, J. G., and Vanderhaeghen, P. (1998) The ephrins and Eph receptors in neural development. *Annu. Rev. Neurosci.* **21,** 309–345
5. Wu, J., and Luo, H. (2005) Recent advances on T-cell regulation by receptor tyrosine kinases. *Curr. Opin. Hematol.* **12,** 292–297
6. Batlle, E., Henderson, J. T., Beghtel, H., van den Born, M. M., Sancho, E., Huls, G., Meeldijk, J., Robertson, J., van de Wetering, M., Pawson, T., and Clevers, H. (2002) β-Catenin and TCF mediate cell positioning in the intestinal epithelium by controlling the expression of EphB/ephrinB. *Cell* **111,** 251–263
7. Dravis, C., Yokoyama, N., Chumley, M. J., Cowan, C. A., Silvany, R. E., Shay, J., Baker, L. A., and Henkemeyer, M. (2004) Bidirectional signaling mediated by ephrin-B2 and EphB2 controls urorectal development. *Dev. Biol.* **271,** 272–290
8. Wang, H. U., Chen, Z. F., and Anderson, D. J. (1998) Molecular distinction and angiogenic interaction between embryonic arteries and veins revealed by ephrin-B2 and its receptor Eph-B4. *Cell* **93,** 741–753
9. Davy, A., Bush, J. O., and Soriano, P. (2006) Inhibition of gap junction communication at ectopic Eph/ephrin boundaries underlies craniofrontonasal syndrome. *PLoS Biol.* **4,** e315
10. Zhao, C., Irie, N., Takada, Y., Shimoda, K., Miyamoto, T., Nishiwaki, T., Suda, T., and Matsuo, K. (2006) Bidirectional ephrinB2-EphB4 signaling controls bone homeostasis. *Cell Metab.* **4,** 111–121
11. Konstantinova, I., Nikolova, G., Ohara-Imaizumi, M., Meda, P., Kucera, T., Zarbalis, K., Wurst, W., Nagamatsu, S., and Lammert, E. (2007) EphA-Ephrin-A-mediated β cell communication regulates insulin secretion from pancreatic islets. *Cell* **129,** 359–370
12. Hashimoto, T., Karasawa, T., Saito, A., Miyauchi, N., Han, G. D., Hayasaka, K., Shimizu, F., and Kawachi, H. (2007) Ephrin-B1 localizes at the slit diaphragm of the glomerular podocyte. *Kidney Int.* **72,** 954–964
13. Dravis, C., Wu, T., Chumley, M. J., Yokoyama, N., Wei, S., Wu, D. K., Marcus, D. C., and Henkemeyer, M. (2007) EphB2 and ephrin-B2 regulate the ionic homeostasis of vestibular endolymph. *Hear. Res.* **223,** 93–104
14. Foo, S. S., Turner, C. J., Adams, S., Compagni, A., Aubyn, D., Kogata, N., Lindblom, P., Shani, M., Zicha, D., and Adams, R. H. (2006) Ephrin-B2 controls cell motility and adhesion during blood-vessel-wall assembly. *Cell* **124,** 161–173
15. Shin, D., Garcia-Cardena, G., Hayashi, S., Gerety, S., Asahara, T., Stavrakis, G., Isner, J., Folkman, J., Gimbrone, M. A., Jr., and Anderson, D. J. (2001) Expression of ephrinB2 identifies a stable genetic difference between arterial and venous vascular smooth muscle as well as endothelial cells, and marks subsets of microvessels at sites of adult neovascularization. *Dev. Biol.* **230,** 139–150
16. Gale, N. W., Baluk, P., Pan, L., Kwan, M., Holash, J., DeChiara, T. M., McDonald, D. M., and Yancopoulos, G. D. (2001) Ephrin-B2 selectively marks arterial vessels and neovascularization sites in the adult, with expression in both endothelial and smooth-muscle cells. *Dev. Biol.* **230,** 151–160
17. Ogita, H., Kunimoto, S., Kamioka, Y., Sawa, H., Masuda, M., and Mochizuki, N. (2003) EphA4-mediated Rho activation via Vsm-RhoGEF expressed specifically in vascular smooth muscle cells. *Circ. Res.* **93,** 23–31
18. Luo, H., Charpentier, T., Wang, X., Qi, S., Han, B., Wu, T., Terra, R., Lamarre, A., and Wu, J. (2011) EFNB1 and EFNB2 proteins regulate thymocyte development, peripheral T cell differentiation and antiviral immune responses and are essential for IL-6 signaling. *J. Biol. Chem.* **286,** 41135–41152
19. Xin, H. B., Deng, K. Y., Rishniw, M., Ji, G., and Kotlikoff, M. I. (2002) Smooth muscle expression of Cre recombinase and eGFP in transgenic mice. *Physiol. Genomics* **10,** 211–215
20. Golovina, V. A., and Blaustein, M. P. (2006) Preparation of primary cultured mesenteric artery smooth muscle cells for fluorescent imaging and physiological studies. *Nat. Protoc.* **1,** 2681–2687
21. Thorin, E., Huang, P. L., Fishman, M. C., and Bevan, J. A. (1998) Nitric oxide inhibits α_2-adrenoceptor-mediated endothelium-dependent vasodilation. *Circ. Res.* **82,** 1323–1329
22. Lavoie, J. L., Lake-Bruse, K. D., and Sigmund, C. D. (2004) Increased blood pressure in transgenic mice expressing both human renin and angiotensinogen in the renal proximal tubule. *Am. J. Physiol. Renal Physiol.* **286,** F965–F971
23. Dumas, P., Pausová, Z., Kren, V., Krenová, D., Pravenec, M., Dumont, M., Ely, D., Turner, M., Sun, Y., Tremblay, J., and Hamet, P. (2000) Contribution of autosomal loci and the Y chromosome to the stress response in rats. *Hypertension* **35,** 568–573
24. Carlson, S. H., Osborn, J. W., and Wyss, J. M. (1998) Hepatic denervation chronically elevates arterial pressure in Wistar-Kyoto rats. *Hypertension* **32,** 46–51
25. Compagni, A., Logan, M., Klein, R., and Adams, R. H. (2003) Control of skeletal patterning by ephrinB1-EphB interactions. *Dev. Cell* **5,** 217–230
26. Somlyo, A. P., and Somlyo, A. V. (1994) Signal transduction and regulation in smooth muscle. *Nature* **372,** 231–236
27. Han, Y. J., Hu, W. Y., Piano, M., and de Lanerolle, P. (2008) Regulation of myosin light chain kinase expression by angiotensin II in hypertension. *Am. J. Hypertens.* **21,** 860–865
28. Kimura, K., Ito, M., Amano, M., Chihara, K., Fukata, Y., Nakafuku, M., Yamamori, B., Feng, J., Nakano, T., Okawa, K., Iwamatsu, A., and Kaibuchi, K. (1996) Regulation of myosin phosphatase by Rho and Rho-associated kinase (Rho-kinase) *Science* **273,** 245–248
29. Tanaka, M., Kamo, T., Ota, S., and Sugimura, H. (2003) Association of Dishevelled with Eph tyrosine kinase receptor and ephrin mediates cell repulsion. *EMBO J.* **22,** 847–858
30. Brückner, K., Pablo Labrador, J., Scheiffele, P., Herb, A., Seeburg, P. H., and Klein, R. (1999) EphrinB ligands recruit GRIP family PDZ adaptor proteins into raft membrane microdomains. *Neuron* **22,** 511–524
31. Lu, Q., Sun, E. E., Klein, R. S., and Flanagan, J. G. (2001) Ephrin-B reverse signaling is mediated by a novel PDZ-RGS protein and selectively inhibits G protein-coupled chemoattraction. *Cell* **105,** 69–79
32. Schulz, T. J., Glaubitz, M., Kuhlow, D., Thierbach, R., Birringer, M., Steinberg, P., Pfeiffer, A. F., and Ristow, M. (2007) Variable expression of Cre recombinase transgenes precludes reliable prediction of tissue-specific gene disruption by tail-biopsy genotyping. *PLoS One* **2,** e1013
33. Ledoux, J., Werner, M. E., Brayden, J. E., and Nelson, M. T. (2006) Calcium-activated potassium channels and the regulation of vascular tone. *Physiology* **21,** 69–78
34. Wamhoff, B. R., Bowles, D. K., and Owens, G. K. (2006) Excitation-transcription coupling in arterial smooth muscle. *Circ. Res.* **98,** 868–878
35. Dong, H., O'Brien, R. J., Fung, E. T., Lanahan, A. A., Worley, P. F., and Huganir, R. L. (1997) GRIP: a synaptic PDZ domain-containing protein that interacts with AMPA receptors. *Nature* **386,** 279–284
36. Su, L. F., Wang, Z., and Garabedian, M. J. (2002) Regulation of GRIP1 and CBP coactivator activity by Rho GDI modulates estrogen receptor transcriptional enhancement. *J. Biol. Chem.* **277,** 37037–37044
37. Ye, B., Liao, D., Zhang, X., Zhang, P., Dong, H., and Huganir, R. L. (2000) GRASP-1: a neuronal RasGEF associated with the AMPA receptor/GRIP complex. *Neuron* **26, 603–617**
38. Luo, H., Wu, Z., Tremblay, J., Thorin, E., Peng, J., Lavoie, J. L., Hu, B., Stoyanova, E., Cloutier, G., Qi, S., Wu, T., Cameron, M., and Wu, J. (2012) Receptor tyrosine kinase EphB6 regulates vascular smooth muscle contractility and modulates blood pressure in concert with sex hormone. *J. Biol. Chem.* **287,** 6819–6829